

Study of electromagnetic radiation by magnons parametrically excited in an antiferromagnet

B. Ya. Kotyuzhanskii, L. A. Prozorova, and L. E. Svistov

Crystallography Institute, USSR Academy of Sciences

(Submitted 23 July 1983)

Zh. Eksp. Teor. Fiz. **86**, 1101–1116 (March 1984)

The properties of electromagnetic radiation from easy-plane antiferromagnetic FeBO_3 and MnCO_3 crystals, in which magnons are parametrically excited, were investigated. The magnons were excited by parallel pumping at a frequency $\omega_p = 2\pi \cdot 35.6$ GHz. The experiments were performed at temperatures 1.2–1.4 K. The radiation was observed in a narrow frequency interval near the frequency $\omega_p/2$. We studied the spectral composition of the radiation as a function of the pump level, the temperature, and the magnetic field. The radiation intensity I was estimated as a function of the number N of the parametric magnons in the sample. It follows from the results that both magnetostatic oscillations and magnons of $k \sim 104\text{--}106 \text{ cm}^{-1}$ emit in FeBO_3 , but only magnetostatic oscillations in MnCO_3 . Stimulated decay of a parametric magnon into a magnon and a long-wave phonon, and simultaneous parametric excitation of magnons and long-wave phonons, are observed.

Ever since parametric excitation of magnons in magnetically ordered substances has been observed experimentally by the methods of perpendicular^{1,2} and parallel³ microwave pumping, the study of the spectral distribution $n(\omega_k, \mathbf{k})$ of parametrically excited magnons has attracted much interest. Here n is the magnon density, i.e., their number per unit volume of the magnet, and ω_k and \mathbf{k} are their frequency and wave number. The reason for this interest is that study of the spectral distribution yields valuable information both on the mechanism of the parametric excitation and on the nature of the stationary state in a system of paramagnetic magnons, particularly on the principal interactions of the magnons with one another, with other elementary excitations such as phonons and nuclear magnons, and with crystal defects.

The fundamental experimental method of parametric excitation of magnons has become the method of parallel pumping (the magnetic microwave field \mathbf{h} is parallel to the static \mathbf{H}), in which the elementary excitation act consists of absorption of a photon (p) with simultaneous production of two magnons (m). The energy and quasimomentum conservation laws impose the following conditions on the frequencies ω_{k_α} and the wave vectors \mathbf{k}_α of the excited magnons ($\alpha = 1, 2$):

$$\omega_p = \omega_{\mathbf{k}_1} + \omega_{\mathbf{k}_2}, \quad \mathbf{k}_p = \mathbf{k}_1 + \mathbf{k}_2. \quad (1)$$

Since $k_p \approx 0$ in the microwave band, it follows from (1) that in excitation of a pair of degenerate oscillations we have

$$\omega_{\mathbf{k}_1} = \omega_{\mathbf{k}_2} = \omega_k = \omega_p/2, \quad \mathbf{k}_1 = -\mathbf{k}_2. \quad (2)$$

The absolute value $k_\alpha = |\mathbf{k}_\alpha|$ is then determined by the magnon spectrum $\omega_k(\mathbf{k})$ and usually ranges from 0 to $10^5 - 10^6 \text{ cm}^{-1}$, depending on the value of the magnetic field.

As a rule, the parametric excitation is identified in experiment by the threshold field h_c at which the absorption of the microwave pump power sets in, by the range of the field H in which this absorption is observed, and by an optimal,

for the development of the process, orientation of the fields \mathbf{h} and \mathbf{H} relative to each other and to the crystal axes. Clearly, all the aforementioned indications are indirect; therefore in some experiments of this type even the interpretation of the observed parametric process is difficult and ambiguous.⁴

Moreover, a still unanswered question is that of the accuracy with which the conditions (2) are satisfied: are the magnons indeed excited only at a frequency ω_k exactly equal to $\omega_p/2$ and the spectral distribution $h(\omega_k)$ has the form of a δ function, or does the excitation span a certain frequency band $\delta\omega_k$?

The fact that the excited magnons have a frequency $\omega_k \sim \omega_p/2$ could be established with low accuracy in experiments in which it was possible to observe a singularity in the relaxation of the paramagnetic magnons at the point of intersection of the magnons spectrum with the phonon spectrum known from other experiments.⁵⁻⁸ The frequency of the excited magnons with $k \approx 10^4\text{--}10^6 \text{ cm}^{-1}$ could be determined more accurately in experiments on Brillouin scattering of light from them.^{9,10} However, the error with which the magnon frequency was determined in these experiments (~ 1 GHz) is still too large for the measurement of $\delta\omega_k$.

The most direct and exact method of determining the spectral distribution of parametric magnons can be a study of the spectral composition of the radiation caused by them. Investigations of this type were performed on iron garnets,¹¹⁻¹⁵ but in all these studies radiation was observed from long-wave magnetostatic oscillations with wave number $k \leq 10^2 \text{ cm}^{-1}$. Such oscillations can receive energy either directly from the pump field (parametric excitation of the natural magnetostatic oscillations of the sample), or from magnons parametrically excited through two-magnon scattering by inhomogeneities in the sample. Emission from homogeneous spin oscillations was observed also following parametric excitation of the nuclear spin system in the antiferromagnetic MnCO_3 and CoMnF_3 .^{16,17}

It must be noted that although two-magnon scattering does not change the magnon frequency, nonetheless the

spectral composition of emission by magnetostatic oscillations can differ substantially, if the oscillations have high Q and the energy transport is effective, from the spectral distribution of parametric magnons. Electromagnetic radiation by parametric magnons with $k = 10^5 - 10^6 \text{ cm}^{-2}$ should, by virtue of the quasimomentum conservation law ($k_m \gg k_p$) be substantially weaker than emission magnetostatic oscillations, and was observed by us earlier in the weak ferromagnet FeBO_3 .¹⁸ We know of no other observation of direct radiation by short-wave magnons.

The present paper is devoted to a more detailed exposition of the results of Ref. 18 and to further study of the properties of emission by parametric magnons in FeBO_3 and MnCO_3 . Parametric excitation of magnons in these substances was investigated in Refs. 19–21, where the basic magnetic parameters of these weak ferromagnets are given.

CALCULATION OF RADIATION INTENSITY

Let us estimate the intensity of the electromagnetic radiation caused by magnons. The structures of FeBO_3 and MnCO_3 are described by the same space group D_{3d}^6 . The thermodynamic potential of a two-sublattice antiferromagnet having this symmetry, with account taken of terms of order not higher than second in the vectors $\mathbf{I} = \mathbf{M}_1 - \mathbf{M}_2$, and $\mathbf{m} = \mathbf{M}_1 + \mathbf{M}_2$, where $\mathbf{M}_{1,2}$ are the sublattice magnetizations ($|\mathbf{M}_1| = |\mathbf{M}_2|$), of the form 22

$$\Phi = \int_V dV \left[\frac{B}{2} m^2 + \frac{a}{2} l_z^2 + d^* (l_x m_y - l_y m_x) + \frac{\alpha^*}{2} \left(\frac{\partial \mathbf{l}}{\partial x_i} \right)^2 - \mathbf{m} \mathbf{H} \right] \quad (3)$$

(the z axis is aligned with the crystal principal axis C).

From the solution of the linearized Landau-Lifshitz equations

$$\begin{aligned} \mathbf{m} &= \gamma \left\{ \left[\mathbf{m} \times \frac{\delta \Phi}{\delta \mathbf{m}} \right] + \left[\mathbf{l} \times \frac{\delta \Phi}{\delta \mathbf{l}} \right] \right\}, \\ \mathbf{l} &= \gamma \left\{ \left[\mathbf{m} \times \frac{\delta \Phi}{\delta \mathbf{l}} \right] + \left[\mathbf{l} \times \frac{\delta \Phi}{\delta \mathbf{m}} \right] \right\} \quad (4) \end{aligned}$$

it follows that the spectrum of the natural oscillations of the vectors

$$\mathbf{l} = \mathbf{l}_0 + \lambda_{\mathbf{k}} \exp[i(\omega_{\mathbf{k}} t - \mathbf{k} \mathbf{r})] \quad \text{and} \quad \mathbf{m} = \mathbf{m}_0 + \mu_{\mathbf{k}} \exp[i(\omega_{\mathbf{k}} t - \mathbf{k} \mathbf{r})]$$

(of plane spin waves) consists of two branches. When $a > 0$ (easy plane) the field \mathbf{H} lies in the basal plane of the crystal (we direct the x axis along \mathbf{H} , then $\mathbf{l}_0 \parallel Y$, $\mathbf{m}_0 \parallel X$, $l_0 = 2|\mathbf{M}_{1,2}|$, $m_0 = (H + d^* l_0)/B$) and in the continuous-medium approximation ($d^{-1} \ll k \ll \pi/a_0$, d is the sample dimension and a_0 is the dimension of the unit cell) these branches are described by the following equations^{23,24}:

$$(\omega_{1\mathbf{k}}/\gamma)^2 = H(H + H_D) + H_{\Delta}^2 + 36H_A^6 H_E \cos 6\varphi + H_{\text{dip}}^2 + \alpha_{\parallel}^2 k_{\parallel}^2 + \alpha_{\perp}^2 k_{\perp}^2, \quad (5)$$

$$(\omega_{2\mathbf{k}}/\gamma)^2 = 2H_A H_E + H_D(H + H_D) + \alpha_{\parallel}^2 k_{\parallel}^2 + \alpha_{\perp}^2 k_{\perp}^2, \quad (6)$$

where γ is the magnetomechanical ratio, $H_E = Bl_0/2$ is the exchange field, $H_p = d^* l_0$ is the Dzyaloshinskii field,

$H_A = al_0$ is the uniaxial anisotropy field, H_{Δ}^6 is the hexagonal-anisotropy field in the basal plane, H_{Δ}^2 is a parameter due to magnetoelastic and hyperfine interactions, H_{dip}^2 is a parameter due to the spin-wave field,²⁵ $\alpha = \alpha^* Bl_0^2$ is the inhomogeneous exchange field (the subscripts \parallel and \perp indicate the direction relative to O_3) and φ is the angle between \mathbf{H} and one of the binary axes in the basal plane. We have included in (5) for completeness the terms with H_{Δ}^2 , H_A^6 , H_{dip}^2 and the anisotropy α . To determine these terms it is necessary to include in the thermodynamic potential (3) additional terms that are of no importance in our problem. The spin oscillations corresponding to the first and second branches of the spectrum are described by different components of the vectors and μ : λ_x, μ_y, μ_z by the first and $\lambda_y, \lambda_z, \mu_x$ by the second.

Under the conditions of the experiment, magnon pairs belonging to the first branch of the spectrum are excited. Each such pair is a standing wave for which, as follows from (4), the relations between the components λ_x, μ_y, μ_z are of the form ($\omega_{1\mathbf{k}}$ will hereafter be designated simply $\omega_{\mathbf{k}}$)

$$\begin{aligned} \lambda_{kx} &= 2A_{\mathbf{k}} \cos(\omega_{\mathbf{k}} t + \psi_{\mathbf{k}}) \cos(\mathbf{k} \mathbf{r} + \theta_{\mathbf{k}}), \\ \mu_{ky} &= -2 \frac{m_0}{l_0} A_{\mathbf{k}} \cos(\omega_{\mathbf{k}} t + \psi_{\mathbf{k}}) \cos(\mathbf{k} \mathbf{r} + \theta_{\mathbf{k}}), \\ \mu_{kz} &= -2 \frac{\omega_{\mathbf{k}}}{\gamma Bl_0} A_{\mathbf{k}} \sin(\omega_{\mathbf{k}} t + \psi_{\mathbf{k}}) \cos(\mathbf{k} \mathbf{r} + \theta_{\mathbf{k}}). \end{aligned} \quad (7)$$

Here $\psi_{\mathbf{k}}$ is the total phase of the pair, is determined by the amplitude and phase of the pump field h , and is the same for all pairs.²⁶ It can therefore be set equal to zero. $\theta_{\mathbf{k}}$ is the phase difference of the pair and remains arbitrary without imposition of additional conditions. Substituting (7) in (3), we can express the amplitudes $A_{\mathbf{k}}$ in terms of the volume densities $n_{\mathbf{k}}$ of the magnons:

$$A_{\mathbf{k}}^2 = 2\hbar\gamma^2 Bl_0^2 n_{\mathbf{k}} / \omega_{\mathbf{k}}. \quad (8)$$

Since the electromagnetic radiation has a wavelength $\lambda_r = c/\omega_{\mathbf{k}} \gg k^{-1}$ (c is the speed of light), the radiation intensity I can be calculated by regarding the sample as a magnetic point dipole with magnetic moment.

$$\mu = \int_V \sum_{\mathbf{k}} \mu_{\mathbf{k}} dV. \quad (9)$$

It can also be shown that the radiation intensity in a waveguide, at optimal coupling, is of the order of the radiation intensity in free space, known to be

$$I = \frac{2}{3c^3} \overline{(\ddot{\mu})^2}. \quad (10)$$

The superior bar means averaging over the period. Hence, assuming that the stationary amplitudes $A_{\mathbf{k}}$ do not depend on the time and that the magnons are excited in a narrow spectral interval ($\delta\omega_{\mathbf{k}}/\omega_{\mathbf{k}}$ and $\delta k/k \ll 1$), we get from (10)

$$\begin{aligned} I &\approx \frac{4\omega_{\mathbf{k}}^4 V^{2/3}}{3c^3 B^2 l_0^2 k^2} \left[B^2 m_0^2 + \left(\frac{\omega_{\mathbf{k}}}{\gamma} \right)^2 \right] \\ &\quad \times \left\{ \sum_{\mathbf{k}} A_{\mathbf{k}}^2 [\sin(kd + \theta_{\mathbf{k}}) - \sin \theta_{\mathbf{k}}]^2 \right. \\ &\quad \left. + \sum_{\mathbf{k}\mathbf{k}'} A_{\mathbf{k}} A_{\mathbf{k}'} \cos[(\omega_{\mathbf{k}} - \omega_{\mathbf{k}'}) t] [\sin(kd + \theta_{\mathbf{k}}) - \sin \theta_{\mathbf{k}}] \right. \\ &\quad \left. \times [\sin(k'd + \theta_{\mathbf{k}'}) - \sin \theta_{\mathbf{k}'}] \right\}. \end{aligned} \quad (11)$$

The factor $[\sin(kd + \theta_k) - \sin\theta_k]$ constitutes at $k \sim 10^4 - 10^5 \text{ cm}^{-1}$ a rapidly oscillating function of the magnetic field H . Its presence in (11) means that the standing spin waves with wavelength $\lambda_k^* = 2\pi/k$, an integer number of which is spanned by sample dimension d , take no part in the radiation, and that only the uncompensated sections of the waves radiate. Doubts may be cast on the validity of the assumption that a standing spin wave extends from one end of the crystal to the other. However, this is the case at any rate in FeBO_3 at helium temperatures, since a size effect is observed in it for parametric excitation of spin waves.²⁷

It can be seen from (11) that the radiation whose average intensity I is specified by the first term (Σ_k), is modulated because of the presence of the second term ($\Sigma_{kk'}$), with a modulation depth ~ 1 and with a frequency $\sim \delta\omega_k$.

Putting by way of estimate $[\sin(kd + \theta_k) - \sin\theta_k]^2 \sim 1/2$, we obtain taking (8) into account

$$I = \frac{4\hbar\gamma^2\omega_k^3 V^{1/2} N}{3c^3 k^2 B} \left[(H+H_D)^2 + \left(\frac{\omega_k}{\gamma}\right)^2 \right] \approx \frac{8\omega_k^4 \mathcal{M}_0 |\Delta\mathcal{M}_0| N}{3c^3 k^2 V^{1/2}}, \quad (12)$$

where $\mathcal{M}_0 = Vm_0$ is the magnetic moment of the sample, $\Delta\mathcal{M}_0$ is its change due to excitation of one magnon, and N is the total number of paramagnetic magnons in the sample.

It can be shown that the last expression in (12) is valid also for ferromagnetic crystals. It follows from (12) that the intensity of the emission from an antiferromagnet having a strong Dzyaloshinskii interaction (such as FeBO_3 , for which $H_0 = 108 \text{ kOe}$) and from a ferromagnet (yttrium iron garnet-YIG) turn out to be of the same order of magnitude if the number of parametric magnons is the same. The reason is that although \mathcal{M}_0 is smaller in antiferromagnets, the quantity

$$\Delta\mathcal{M}_0 = -\frac{\partial \mathcal{E}_k}{\partial H} = -\hbar \frac{\partial \omega_k}{\partial H} = -\frac{g\gamma(2H+H_D)}{2\omega_k} \mu_B \quad (13)$$

(g is the spectroscopic splitting factor and μ_B is the Bohr magneton) may turn out to be substantially larger.²⁸

PROCEDURE AND SAMPLES

The emission of electromagnetic waves by parametric magnons was investigated with the setup whose block diagram is shown in Fig. 1. The basic part of the setup was a flow-through microwave spectrometer. The cylindrical cavity was so tuned that its H_{012} mode coincided with the pump frequency ω_p . The sample was placed in the exit coupling port of the cavity, symmetric relative to its wall (which is 0.5 mm thick). Thus, part of the sample was located inside the resonator, at the antinode of the microwave magnetic field \mathbf{h} , and the other in a standard 1.5-cm waveguide ($11 \times 5.5 \text{ mm}$). The sample was fastened with the aid of a cigarette-paper container. This fastening method made it possible to preserve the high sample acoustic Q needed for the observation of certain phenomena, and avoid the elastic tensions that accompany its cooling and influence strongly the spectrum of the magnons in FeBO_3 . The fields \mathbf{h} and \mathbf{H} were in the basal plane of the crystal, and the direction of \mathbf{H} in this plane could vary in the course of the experiment. The principal

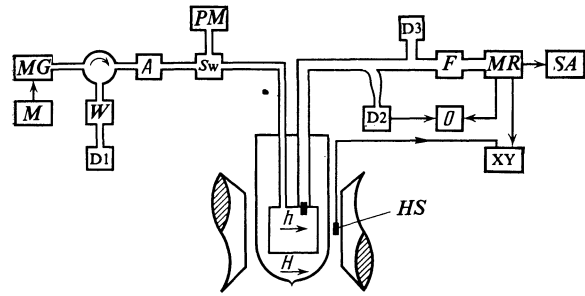


FIG. 1. Block diagram of setup: MG —magnetron generator, M —modulator, W —wavemeter, $D_{1,2,3}$ —detectors, A —attenuator, Sw —transfer switch, PM —power meter, HS —Hall sensor, F —filter, MR —measuring receiver, O —oscilloscope, SA —spectrum analyzer, XY — x - y recorder.

experiments were performed at small values of the angle between \mathbf{h} and \mathbf{H} ($\lesssim 30^\circ$). In this case the magnons were excited by the \mathbf{h} component parallel to the static field.

The microwave pumping was with a cw magnetron oscillator of frequency $\omega_p = 2\pi \cdot 35.6 \text{ GHz}$ and power $\sim 10 \text{ W}$. In some experiments the magnetron operated in a long-pulse regime obtained by modulating its anode voltage. The pulse duration could be varied from 0.01 to 1 msec, and power was the 50 Hz mains. The microwave power fed to the microwave cavity was measured with a thermistor power meter of $\sim 20\%$ accuracy.

The microwave signal from the cavity was split by 1.5-cm-band directional coupler into two beams. The diverted beam passed through an 8-mm-band waveguide ($7.2 \times 3.4 \text{ mm}$), beyond cutoff at the frequency $\omega_p/2$, to a square-law crystal detector. The voltage from this detector proportional to the square h^2 of the microwave pump field at the sample, was fed to the first beam of a two-beam oscilloscope. The signal passing straight through the coupler was applied to the input of a P5-14A superheterodyne measuring receiver through a filter that attenuated its ω_p frequency component by $\sim 40 \text{ dB}$. The maximum receiver sensitivity was $\sim 10^{14} \text{ W}$. The receiver output voltage, proportional to the power of the signal of frequency $\approx \omega_p/2$ from the cavity, was applied to the second oscilloscope beam and its dependence on the magnetic field H was plotted with an $x - y$ recorder.

The bandwidth of the investigated radiation at not too high an excitation of the parametric magnons was narrower than the pass band of the receiver ($\approx 10 \text{ MHz}$), so that its spectral composition could be studied by analyzing the voltage of the second intermediate frequency of the receiver ($\approx 30 \text{ MHz}$). A spectrum analyzer S4-45 with a pass band 3 kHz was used for this purpose.

The measurements were performed in the temperature interval 1.2–4.2 K. To improve the heat removal from the sample, the cavity with the sample were filled with liquid helium. The temperature was determined from the saturated-vapor pressure to within $\pm 0.05 \text{ K}$.

The FeBO_3 and MnCO_3 single-crystal samples were cylinders of $\sim 2 \text{ mm}$ diameter and $\sim 3 \text{ mm}$ height. The cylinder axis coincided with the principal axis of the crystal, and the bases were growth planes that coincided with the basal plane.

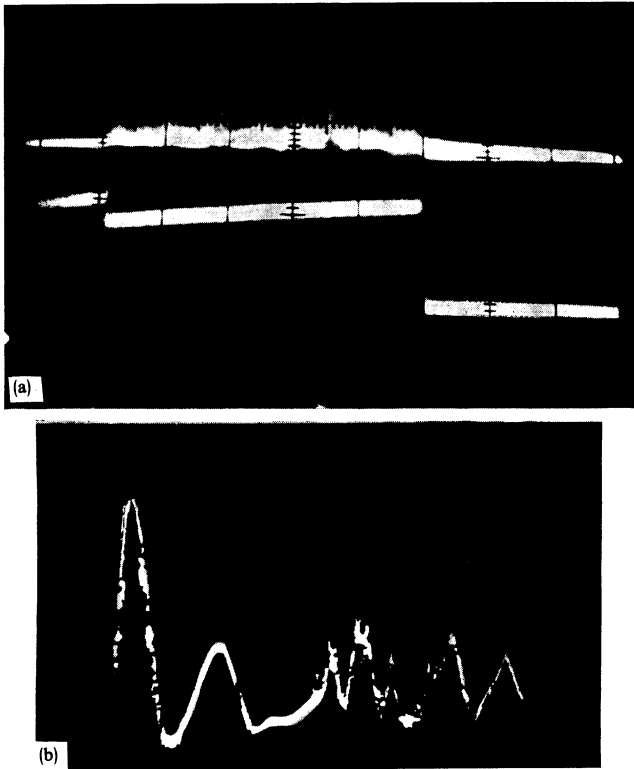


FIG. 2. Oscillogram of emission signal at $h \gtrsim h_{c1}$, $T = 1.2$ K, $H = 300$ Oe; a—upper beam—signal from receiver, lower—from detector D_2 , pump pulse duration 1 msec; b—signal from receiver, sweep time 20 μ sec.

MEASUREMENT RESULTS

1. FeBO_3

The experiments have established that besides the drop on the pump pulse of frequency ω_p , which attests to the parametric buildup of the magnon oscillations, radiation appears on the sample at a frequency $\omega_p/2$. The corresponding oscillograms are shown in Fig. 2. The radiation intensity I depended randomly on the time. As seen from Fig. 2, the oscillogram of the output signal of the receiver took the form of spikes having a characteristic duration τ .

It is known¹⁹ that in FeBO_3 at helium temperature the parametric excitation is hard, i.e., it is characterized by two threshold fields, for the start (h_{c1}) and for the end (h_{c2}) of the process ($h_{c1} > h_{c2}$). Investigations in the cw pumping regime have shown that the radiation, as well as the excitation stops at $h = h_{c2}$. At near-unity values of the pump level $\xi = h/h_{c2}$ the radiation bandwidth $\delta\omega$ was $2\pi \cdot 40$ kHz and was apparently determined by a parasitic deviation of the magnetron frequency, which had the same bandwidth $\sim 2\pi \cdot 40$ kHz. The spectral band of the radiation broadened with increasing pump power.

The center of the radiation band was at $\omega_p/2$ accurate to $\pm 2\pi \cdot 20$ kHz. This was determined by applying to the receiver input, simultaneously with the radiation signal, a signal from a supplementary klystron microwave oscillator tuned in such a way that its second harmonic coincided with the pump frequency. The klystron was turned to zero voltage beats with the microwave detector on which the klystron and magnetron signals were incident. Within the limits

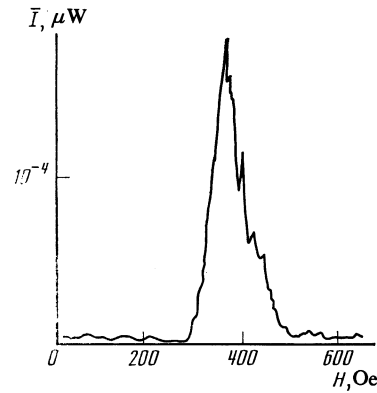


FIG. 3. Dependence of the average radiation intensity I at the receiver input on the magnetic field H ; $\xi^2 \sim 10$, $T = 1.2$ K.

of the measurement error of the frequency connected with the parasitic deviation of the klystron and magnetron frequencies, the latter two frequencies were equal.

The radiation was observed in the entire range of the magnetic field H (from 0 to ~ 500 Oe) in which parametric excitation of the magnons took place. Figure 3 shows the automatically plotted dependence of the receiver-output voltage, proportional to the time-averaged radiation intensity \bar{I} , on the magnetic field H at a constant pump power corresponding to $\xi^2 \approx 10$. It can be seen from Fig. 3 that in a certain field region whose width is close to the width of the band of the magnetostatic modes ($4M_s = 225$ G, M_s is the spontaneous magnetization), the radiation intensity increases steeply. The range of variation of the intensity was ~ 20 dB. In a field H corresponding to the maximum, the radiation intensity \bar{I} at $h = h_{c1}$ and $T = 4.2$ K was $\sim 10^{-10}$ W. The microwave power absorbed in this case at the pump frequency ω_p was $P = 2 \times 10^{-3}$ W.

The intensity of the radiation from magnons with large k was of the same order as the integral noise power of the receiver, and could therefore not be recorded with the plotter. The radiation intensity was measured in this case with a spectrum analyzer.

When the direction of the field \mathbf{H} was varied in the basal plane of the crystal, the hexagonal anisotropy of the intensity-peak position was observed. The shift of the intensity peak corresponded then to a shift of the antiferromagnetic resonance line at the frequency $\frac{1}{2}\omega_p$, which was recorded by us simultaneously with the x - y recorder.

At not too low pump levels ξ the spectral radiation characteristics were also found to depend substantially on the \mathbf{H} direction in the basal plane relative to the crystallographic axes. Figure 4 shows photographs of the spectrum on the analyzer screen; they demonstrate the change of the radiation spectrum with increasing pump level when \mathbf{H} is perpendicular to the binary axis. Initially, at $\xi \lesssim 10$, the spectrum broadens smoothly with increasing ξ . Figure 5 shows plots of the radiation spectrum width $\delta\omega_{0.1}$ vs ξ , obtained in this ξ interval at two values of the temperature in a field $H = 380$ Oe, where the emission intensity is a maximum. The spectrum width $\delta\omega_{0.1}$ was measured at the 0.1 intensity level. At other values of the static field H the width of the

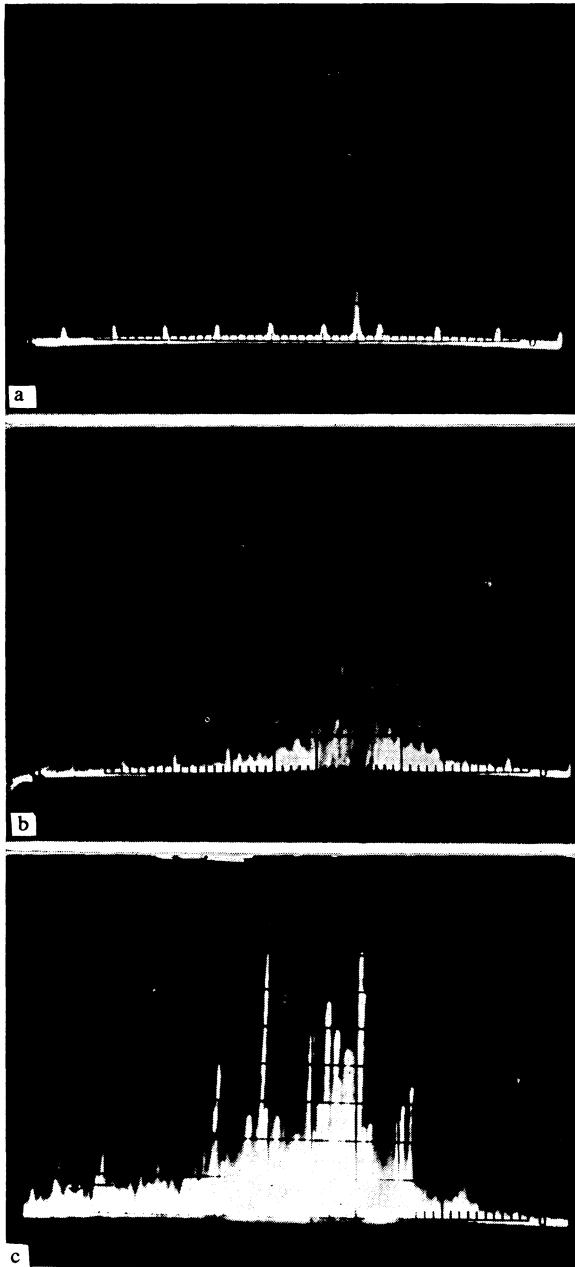


FIG. 4. Change of emission spectrum with increase of the pump level ξ : a— $\xi \sim 1.5$, b— ~ 5 , c— ~ 15 ; H perpendicular to the binary axis, $T = 1.2$ K, $H = 300$ Oe. The spikes in Figs. a and b mark 1 MHz frequency intervals.

emission spectrum also increased in proportion to $(\xi - 1)$: $\delta\omega_{0.1} = \beta (\xi - 1)$. The dependence of the proportionality coefficient β on the static field H is shown in Fig. 6. We note that when $\delta\omega$ was varied the characteristic duration τ of the emission spikes (see Fig. 2) also changed and amounted to $\sim \delta\omega^{-1}$.

With further increase of ξ the emission spectrum broadened jumpwise at a certain threshold $h = h_c^*$ that depended on the temperature and on H , and became wider than the pass band of the receiver: $\delta\omega \sim 2\pi (15 - 20)$ MHz (see Fig. 4c). The ratio h_c^*/h_{c2} was ~ 10 . At $h > h_c^*$ individual well-separated emission bands (satellites) showed up above the

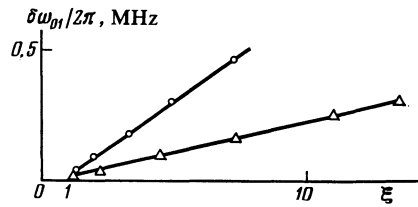


FIG. 5. Dependence of the spectral emission width $\delta\omega_{0.1}$, measured at the 0.1 intensity level, on the pump level ξ at $H = 380$ Oe; Δ — $T = 1.2$ K, O — 4.2 K.

broad emission line. The satellite frequency shift relative to the central frequency $\frac{1}{2}\omega_p$ was independent of the small change ($\sim 2\pi \cdot 3$ MHz within the resonance curve of the cavity) of the pump frequency, of the value of H , and of the temperature, and was a multiple of a certain set of frequencies Ω_i in the megahertz band.

The number of the different frequencies in the set depended on the method of fastening the sample. In the case of "free" fastening in a cigarette-paper container, several frequencies Ω_i were observed, two of which, $2\pi \cdot 0.9$ and $2\pi \cdot 1.2$ MHz, corresponded to the most noticeable satellites. If the sample was secured in the coupling port of the cavity with BF glue, only the frequency $\Omega = 2\pi \cdot 0.9$ remained. The appearance of the satellites was simultaneously accompanied by modulation, at frequencies Ω_i of the pump-frequency microwave signal passing through the cavity and of the emission signal at half that frequency. This could be verified by analyzing the voltages from the microwave detectors of the corresponding bands. We note that the spectrum width directly preceding the jumplike emission-spectrum broadening occurring when the microwave field h at the sample increases to H_c^* was $\sim 2\pi \cdot 1$ MHz, i.e., close to the lowest of the frequencies Ω_i .

In the case when the field H is directed along the binary axis of the crystal, the emission-spectrum change on increase of the pump level differs qualitatively from the preceding

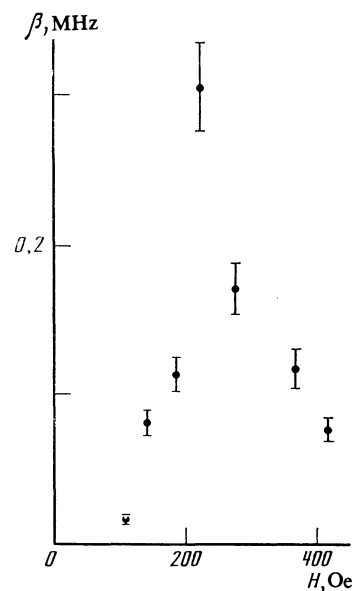


FIG. 6. Dependence of proportionality coefficient $\beta = \delta\omega_{0.1}/(\xi - 1)$ on the magnetic field H at $T = 1.2$ K.

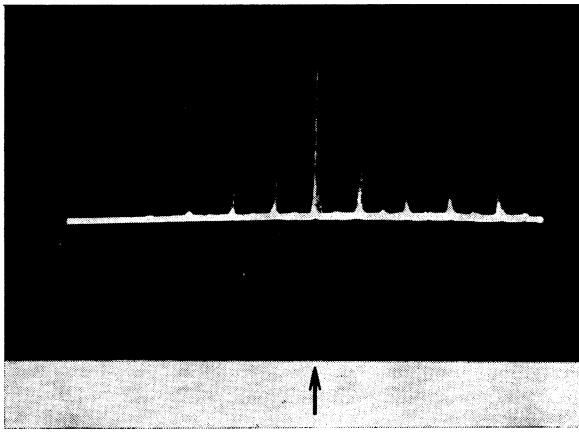


FIG. 7. Emission spectrum for H parallel to the binary axis; $\xi \sim 2.5$; $T = 1.2$ K; $H = 300$ Oe; the arrow marks the frequency $\omega_p/2$.

case. First, at $\xi \lesssim 1.5$, one emission line of frequency $\frac{1}{2}\omega_p$ was likewise observed (see Fig. 4a). With further increase of ξ , satellites appeared and were symmetric about the first fundamental emission line. The number of satellites increased with increasing ξ and reached ~ 20 at $\xi \sim 10$. The emission spectrum at $\xi \sim 2$ is shown in Fig. 7. The spacings of the individual emission lines were $\Omega = 2\pi \cdot 0.9$ or $2\pi \cdot 1.8$ MHz, depending on the pump level and on the value of H . Just as for H perpendicular to the binary axis, the microwave signals from the cavity were modulated at a frequency Ω . The width of each emission line increased monotonically with increasing ξ . At $\xi \sim 10$, in analogy with the foregoing, the emission spectrum broadened jumpwise to $\delta\omega \sim 2\pi(15 - 20)$ MHz.

Notice should be taken of a fact, important in our opinion, that in certain ranges of the angle φ , of the magnetic field H , and of the pump level ξ (up to the second threshold, i.e., at $h < h_c^*$) the intensity of the satellites closest to the fundamental emission line exceeded the intensity of the latter (see Fig. 8).

2. $MnCO_3$

In this crystal, too, emission was observed following parametric excitation of the magnons, but its characteristics and the conditions under which it is observed differ substantially from those described above for $FeBO_3$. The emission was recorded in several narrow intervals of the magnetic field H . The dependence of the average emission intensity on the field H consisted of lines (from one to three, depending on the placement of the crystal in the coupling port) of width ~ 10 – 20 Oe. The automatically plotted absorption curve, corresponding to antiferromagnetic resonance at the frequency $\frac{1}{2}\omega_p$, was also split into the same number of lines, but broader ones. The number of lines decreased when the fraction of the sample located in the cavity increased. Each emission line was contained inside the corresponding absorption line. All the emission lines were located near the field H_0 in which magnons with $k = 0$ were excited. The value of H_0 is obtained by substituting $k = 0$ in Eq. (5) ($h_0 = 4.2$ kOe at $T = 1.2$ K).

Just as in $FeBO_3$ the parametric excitation of the mag-

nons in $MnCO_3$ is hard.²¹ We shall therefore reckon the pump level from the threshold $h_{c2} : \xi h / h_{c2}$. Experiment has shown that in the pulsed pumping regime the emission appears directly past the pulse drop that reveals the magnon excitation. In the cw regime, the emission was observed at arbitrary $\xi > 1$. The emission was recorded in a frequency band $\omega = 1/2\omega_p \pm 2\pi \cdot 0.3$ MHz. The width of the emission band was independent of the temperature and of the pump level in the ξ interval from 1 to 4.

The time evolution of the emission was investigated in the pulsed pumping regime. It was found that the emission intensity varies with time. The first emission spike was 100 μ sec long. The emission intensity then decreased and became noiselike. By varying the pump level and the pulse repetition frequencies and durations, and also by changing slightly the frequencies of the pump ($\sim 2\pi \cdot 3$ MHz) and of the magnetic field H , it was possible to change somewhat (by ~ 200 μ sec) the time from the drop on the pulse to the vertex of the first emission spike. The character of the foregoing dependences indicates that the crystal or its nuclear subsystem is heated when the magnon frequency is correspondingly changed, owing to the term H_{Δ}^2 in (5) which is equal to $5.8 T^{-1}$ kOe² for $MnCO_3$.²⁰ The maximum temperature rise above that of the helium bath was ~ 0.3 K. The presence of the rise is confirmed also by a shift of the antiferromagnetic resonance line. Measurements performed with different pump pulse repetition frequencies have shown that the cooling time is ~ 500 μ sec.

DISCUSSION OF RESULTS

1. $FeBO_3$

It follows from the results of our research, in our opinion, that one can observe emission of electromagnetic waves both by magnetostatic oscillations and directly by parametrically excited magnons with $k \sim 10^4 - 10^5$ cm⁻¹. This statement is based on the fact that resonant excitation of magnetostatic modes of a sample at a frequency $\frac{1}{2}\omega_p$ and hence emission by these modes is possible only in a certain magnetic-field interval $\Delta H \sim 4\pi M_s$. It is precisely in this field interval that an abrupt increase of the emission intensi-

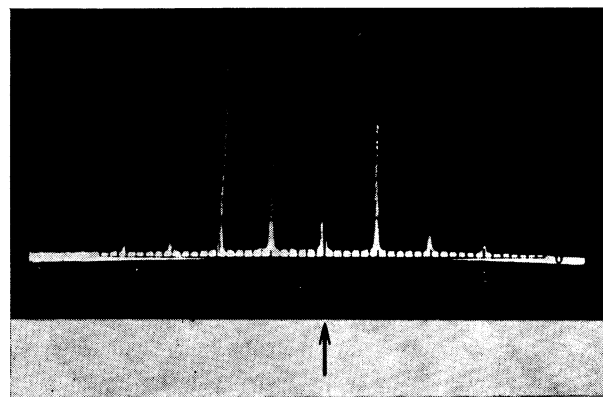


FIG. 8. Realization of the emission spectrum when the satellite intensity exceeded the intensity of the fundamental line; $T = 1.2$ K; the arrow marks the frequency $\omega_p/2$.

ty is observed (see Fig. 3), an increase thus attributable to magnetostatic oscillations.

On the other hand, the intensity of emission by magnons with $k \sim 10^5 \text{ cm}^{-1}$ can be estimated with the aid of (12) and with an expression that connects the microwave pump power P absorbed by the sample with the total number N of the magnons:

$$N = P / \hbar \omega_k \Delta \omega_k, \quad (14)$$

where $\Delta \omega_k$ is the magnon relaxation parameter. Using the value $\Delta \omega_k = 2\pi \cdot 3 \text{ MHz}$ obtained in Ref. 19 at $T = 4.2 \text{ K}$ for $P \sim 10^{-3} \text{ W}$, we get $\bar{I} \sim 10^{-10} \text{ W}$, which is even approximately two decades larger than the experimentally observed value. It can therefore be assumed that the emission outside the intensity peak comes from magnons with large k . The discrepancy between the observed and calculated values of \bar{I} is probably due to the approximate character of the theoretical estimate. In particular, no account was taken of the coupling of the sample to the waveguide channel (the emission is produced by the part of the sample located in the cavity, but enters the waveguide through a narrow coupling port), or of the losses in the latter.

We note also that oscillations with small k have, as follows from (12), larger radiative losses and hence a stronger excitation field h_c , other conditions being equal. Therefore, since the emission spectrum has no singularities in the field interval where the magnetostatic oscillations emit, it can be assumed that under the experimental conditions the energy was fed to these oscillations from the parametric magnons via two-magnon scattering by defects, without a change in the spectral composition, so that the emission spectrum $\bar{I}(\omega)$ coincides in the entire interval of the fields \mathbf{H} with the spectral distribution $n(\omega_k)$ of the parametric magnons. Accordingly $\delta\omega = \delta\omega_k$.

The spectral distribution of parametrically excited magnons was investigated experimentally^{14,15} in YIG and theoretically¹⁵ in the case of a ferromagnetic crystal. In Ref. 15 are indicated the causes of the appearance of a nonzero $\delta\omega_k$, which undoubtedly takes place in an antiferromagnet. These are the intrinsic and thermal noises due respectively to interaction of the parametrically excited magnons with one another and with thermal oscillations. It is important here that the excited magnons are distributed over a large number of states with different k , so that the fluctuation δn_k of the number of magnons in each state is comparable with n_k . It is also pointed out there that scattering by inhomogeneities influences substantially the value of $\delta\omega_k$.

Since there is no theory that describes the spectral distribution of the parametric magnons in an antiferromagnet, we can only compare the values of $\delta\omega_k$ obtained for FeBO₃ and YIG. At the same pump level ξ , the value of $\delta\omega_k$ is more than a decade larger in FeBO₃ than in YIG, although the relaxation parameters $\Delta\omega_k$ for the two substances are close. Since the values of $\delta\omega_k$ given in Refs. 14 and 15 differ by two decades, we took the value of $\delta\omega_k$ from the later Ref. 15. The noisy character of the spectrum broadening agrees with the noisy character of the emission (see Fig. 2).

We proceed to discuss the nature of the jumplike in-

crease of $\delta\omega_k$ that occurs when the field h at the sample reaches the threshold value h_0^* . In Ref. 19 was reported an effect observed in FeBO₃ and named "secondary instability" of parametrically excited magnons. The effect manifests itself as follows: the oscillogram of a signal from a detector located past the microwave cavity showed, when the microwave field h reached a threshold, a "backward jump" corresponding to a decrease of the pump power absorbed by the sample. The backward jump was immediately followed by development of oscillations of the signal from this detector, with a very stable frequency $\sim 2\pi \cdot 2 \text{ MHz}$. As a result of the study of the secondary instability it was proposed in Ref. 19 that when the amplitude A_k of the parametric spin wave reaches a certain critical value A_k^* (or a magnon density $n_k = n_k^*$), the magnon decay leads to an avalanche-like increase of the amplitude of the secondary waves, which turn out in this case to be long-wave elastic oscillations—a natural elastic mode of the sample.

The experiments have demonstrated that the development of the secondary instability and the jumplike broadening $\delta\omega_k$ of the magnon spectrum occur at equal field thresholds $h = h_c^*$ and are thus manifestations of one and the same effect.

Let us discuss the possible processes that lead to excitation of the long-wave elastic oscillations in the sample. First, as already indicated, these may be decays of the parametric magnons. The most probable are processes in which the smallest number of particles participates. In this case this is a three-particle decay of the parametric magnon m_p (with frequency ω_k) into a magnon $m_-(\omega_{k-})$ and a phonon $ph(\Omega_q)$:

$$m_p \rightarrow m_- + ph. \quad (15)$$

It is important here that although in FeBO₃ this process is allowed by the energy and quasimomentum conservation laws in an interval of fields \mathbf{H} where the magnon velocity $s_k = \partial\omega_k / \partial\mathbf{k}$ exceeds that of sound ($v < s = \alpha\gamma$, s is the magnon speed limit), when phonons having a wavelength on the order of the sample size the quasimomentum conservation law can be disregarded, since it is satisfied accurate to $\Delta k \sim 2\pi/d$ in a crystal of finite size. In the upshot we get for the process (15)

$$\omega_k = \omega_{k-} + \Omega_q. \quad (16)$$

The increase of the phonon density n_q as a result of such a decay can either have a threshold at $n_k = n_k^*$ ($\Delta\omega_{k-}$, $\Delta\Omega_q$), if the magnons m_- or the phonons ph are not independently produced through other processes, or may be thresholdless in the opposite case, for example when m_- is also parametric. In both cases the process is stimulated, but the secondary instability in the rigorous sense is only the decay with the threshold.

Second, the long-wave phonons can be excited parametrically directly by microwave pumping ω_p , via multiparticle processes, e.g.,

$$p \rightarrow m_1 + m_2 + ph \quad (17)$$

and

$$p \rightarrow m_1 + m_2 + ph_1 + ph_2. \quad (18)$$

These processes also have thresholds.

It must be noted that regardless of the mechanism that excites the long-wave phonons Ω_q , their successive interactions first with the parametric magnons ω_k , and then with the magnons of second, etc., generations, the magnons excited in the sample have the frequencies

$$\omega_{kN} = \omega_k \pm N\Omega_q, \quad (19)$$

where N is a natural number. Of course, the density n_{kN} of magnons excited in this manner will decrease with increasing N .

The investigations have made it clear that the gist of the secondary-instability effect is the following. When the pump level ξ is raised, the bandwidth of the parametrically excited magnons increases (see Figs. 4a and 4b). When this band becomes equal to one of the frequencies of the natural elastic oscillations of the sample, the thresholdless parametric magnon decay (15) takes place, and, in accordance with (19), the spectrum of the excited magnons broadens jumpwise (see Fig. 4c).

That a connection exists between the observed effect and the excitation of the natural modes of the elastic oscillations of the sample is indicated by the following: the appearance of satellites simultaneously with modulations of the pump power at frequencies Ω_i , the correspondence of the band of the frequencies Ω_i to the interval that contains the frequencies of the natural oscillations with wavelength on the order of the sample dimensions ($\Omega_i \sim 2\pi \cdot 1$ MHz, $d \sim 0.2$ cm, $v \sim 5 \times 10^5$ cm/sec), the high stability of the oscillation frequencies Ω_i when the external conditions are constant (the long-term stability was ~ 100 Hz), the very weak dependence of Ω_i on the pump level and on the temperature, and the variation of the set of frequencies Ω_i with change of the sample-fastening method. The observed increase of the frequency of the oscillation with $\Omega = 2\pi \cdot 0.9$ MHz by $\sim 2\pi \cdot 20$ kHz when ξ is increased by three times is apparently explained by the nonlinearity of the elastic oscillations, which may turn out to be appreciable because of their connection with the spin oscillations.³⁰ The set of excited elastic modes and the amplitude of the corresponding oscillations are determined by the magnetoelastic coupling of the given mode with the parametric magnons and by its relaxation.

Thus, the effect called secondary instability in Ref. 19 is nothing of this kind. Its thresholdlike attributes (abrupt broadening of the spectrum, change of the power absorbed by the sample, and increase in the number of phonons) are the result of the existence of a critical bandwidth $\delta\omega_k^* = \Omega_{i_{\min}}$ of the parametric magnons, on reaching of which the stimulated thresholdless decay (15) sets in. In turn, since $\delta\omega_k$ increases with increasing h , it follows that $\delta\omega_k^*$ corresponds to $h = h_c^*$.

Nevertheless, except for the case when the static magnetic field \mathbf{H} is applied in the basal plane of the crystal in a direction close to perpendicular to the binary axis, at least one more mechanism for the excitation of elastic oscillations is observed (see Fig. 7). In this case the elastic oscillations and the satellites appear prior to the secondary instability,

when $\delta\omega_k$ is still considerably less than $\Omega_{i_{\min}}$, and their appearance causes no jumplike broadening of the magnon spectrum. Such a mechanism can be either the decay (15) with a threshold, or else also the thresholdlike parametric excitation (17) or (18).

From the fact that under certain experimental conditions a situation arises wherein the intensity $\bar{I}_{k\pm}$ of the fundamental emission line of the satellites exceeds the intensity \bar{I}_k of the fundamental line (see Fig. 8) it follows, in our opinion, that what is observed is the parametric process (17) or (18) of simultaneous excitation of magnons and long-wave phonons by a microwave pump ω_p . Otherwise if the magnons with frequencies $\omega_{k\pm} = \omega_k \pm \Omega_q$ corresponding to these satellites were produced via decay of parametric magnons $\omega_k = \omega_p/2$ followed by coalescence of the phonons Ω_q with the magnons ω_k [see (19)], the densities $n_{k\pm}$ of the secondary magnons should be smaller than n_k , since the magnon frequencies ω_k and $\omega_{k\pm}$ (meaning also their relaxation parameters $\Delta\omega_k$ and $\Delta\omega_{k\pm}$) are practically equal; consequently $\bar{I}_{k\pm} < \bar{I}_k$. To determine which of the processes (17) and (18) is observed, additional investigations are necessary.

The arguments advanced do not exclude the possibility of a decay (15) with a threshold takes place in parallel with the parametric process (17) or (18). Under conditions when both these processes are possible, however, the experiments performed do not permit an unambiguous identification of the decay process.

Excitation of natural elastic oscillation of the sample upon parametric excitation of magnons was observed also in MnCO_3 .³¹ In that reference the elastic oscillations were recorded directly with a piezoelectric sensor, and the presence of magnons of frequency $\omega_{k+} = \omega_k + \Omega_q$ was indirectly determined from the change of the kinetics of excitation of the magnons by a second pump at a frequency $\omega_{p2} = \omega_p + 2\Omega_q$. It was shown that the magnons with frequencies intermediate between ω_k and $\omega_{k\pm}$ are not excited to a noticeable level. Just as in the present study, oscillations of the absorbed pump power were observed in Ref. 31 upon excitation of elastic oscillations. On the basis of the results it was concluded in Ref. 31 that in MnCO_3 the elastic oscillations are excited by the decay (15) with threshold.

It must be pointed out that the noticeable hexagonal anisotropy of the spectral distribution of the parametric magnons, revealed by us, agrees with the hexagonal anisotropy of the above-threshold susceptibility χ'' , noted on parametric excitation of magnons in this substance.³² We assume that these properties are determined by the anisotropy of the magnetoelastic interaction that plays an important role in the formation of the stationary above-threshold state.^{28,32}

2. MnCO_3

It follows from the results of the investigations that in this substance radiation is observed only from magnetostatic oscillations. The splitting of the resonant absorption curve into several lines is due apparently to the poor quality of the crystal and to the non-uniformity of the microwave field \mathbf{h} in the sample. We believe that the presence of several emission lines is not due to excitation of different magnetostatic

modes, but is determined by the same factors.

The relatively weak emission intensity ($\bar{I} \sim 10^{-9}$ W at an absorbed pump power $P \sim 10^{-3}$ W) and the appearance of radiation directly past the excitation threshold $\hbar\epsilon_2$ are grounds for assuming that the magnetostatic oscillations are not excited directly, but that the energy is fed to them via two-magnon scattering of parametric magnons with larger k .

The fact that we did not succeed in recording direct radiation from magnons with $k \sim 10^5 \text{ cm}^{-1}$ can be attributed to the small H_D in this substance. According to (12) $\bar{I} \propto H_D^2$, and in MnCO_3 we have $H_D = 4.4 \text{ kOe}$, i.e., approximately 20 times smaller than in FeBO_3 . It is also possible that the intensity and other characteristics of the emission depend on the nature of the stationary state in the system of parametric magnons. In MnCO_3 it is determined by the phase mechanism that limits the number of magnons,³³ and in FeBO_3 by the nonlinear-damping mechanism.³²

The authors are deeply grateful to A. S. Borovik-Romanov and I. S. Zheludev for constant interest, and to A. I. Smirnov, A. S. Mikhaïlov, and A. V. Chubukov for helpful discussions.

¹R. W. Damon, *Rev. Mod. Phys.* **25**, 239 (1953).

²N. Bloembergen and S. Wang, *Phys. Rev.* **93**, 72 (1954).

³E. Schlomann, J. Green, and U. Milano, *J. Appl. Phys.* **32S**, 368S (1961).

⁴V. I. Ozhogin and A. Yu. Yakubovskii, *Zh. Eksp. Teor. Fiz.* **57**, 287 (1974) [*sic*].

⁵E. H. Turner, *Phys. Rev. Lett.* **5**, 100 (1960).

⁶R. L. Comstock and R. C. LeCraw, *Phys. Rev. Lett.* **10**, 219 (1963).

⁷M. H. Seavey, *ibid.* **23**, 132 (1960).

⁸B. Ya. Kotyuzhanskii and L. A. Prozorova, *Pis'ma Zh. Eksp. Teor. Fiz.* **12**, 105 (1970) [*sic*]; *Zh. Eksp. Teor. Fiz.* **65**, 2470 (1973) [*Sov. Phys. JETP* **38**, 1233 (1974)].

⁹V. N. Venitskii, V. V. Eremenko, and E. V. Matyushkin, *Pis'ma Zh.*

Eksp. Teor. Fiz. **27**, 239 (1978) [*JETP Lett.* **27**, 222 (1978)].

¹⁰V. G. Zhotikov and N. M. Kreines, *Zh. Eksp. Teor. Fiz.* **77**, 2486 (1979) [*Sov. Phys. JETP* **50**, 1202 (1979)].

¹¹A. V. Vashkovskii and Ya. A. Monosov, *Radiotekh. Elektron.* **11**, 167 (1966).

¹²A. V. Vashkovskii and Ya. A. Monosov, *ibid.* **12**, 1392 (1967).

¹³N. N. Kiryukhin and Ya. A. Monosov, *Fiz. Tverd. Tela (Leningrad)* **13**, 1944 (1971) [*sic*].

¹⁴N. G. Kutovoi and G. A. Melkov, *ibid.* **17**, 958 (1975) [**17**, 1273 (1975)].

¹⁵I. V. Krutsenko, V. S. L'vov, and G. A. Melkov, *Zh. Eksp. Teor. Fiz.* **75**, 1114 (1978) [*Sov. Phys. JETP* **48**, 561 (1978)].

¹⁶Yu. M. Bun'kov and T. V. Maksimchuk, *Proc. 20th All-Union Conf on Low Temp. Phys., Moscow, 1979, part II*, p. 62.

¹⁷S. A. Govorkov and V. A. Tulin, *Pis'ma Zh. Eksp. Teor. Fiz.* **33**, 445 (1981) [*JETP Lett.* **33**, 428 (1981)].

¹⁸B. Ya. Kotyuzhanskii, L. A. Prozorova, and L. E. Svistov, *ibid.* **37**, 586 (1983) [**37**, 700 (1982)].

¹⁹B. Ya. Kotyuzhanskii and L. A. Prozorova, *Zh. Eksp. Teor. Fiz.* **81**, 1913 (1981) [*Sov. Phys. JETP* **54**, 1013 (1981)].

²⁰B. Ya. Kotyuzhanskii and L. A. Prozorova, *ibid.* **62**, 2100 (1972) [*sic*].

²¹B. Ya. Kotyuzhanskii, *ibid.* **63**, 2205 (1972) [**36**, 1165 (1973)].

²²I. E. Dzyaloshinskii, *ibid.* **32**, 1547 (1957) [**5**, 1259 (1957)].

²³A. S. Borovik-Romanov, *ibid.* **36**, 766 (1959) [**9**, 539 (1959)]. E. A. Turov, *ibid.* p. 1254 [890].

²⁴E. A. Turov and N. G. Guseinov, *ibid.* **38**, 1326 (1960) [**11**, 955 (1960)].

²⁵V. I. Ozhogin, *ibid.* **48**, 1307 (1965) [**21**, 874 (1966)].

²⁶V. E. Zakharov, V. S. L'vov, and S. S. Starobinets, *Usp. Fiz. Nauk* **114**, 609 (1974) [*Sov. Phys. Usp.* **17**, 896 (1975)].

²⁷B. Ya. Kotyuzhanskii and L. A. Prozorova, *Pis'ma Zh. Eksp. Teor. Fiz.* **32**, 254 (1980) [*JETP* **32**, 235 (1980)].

²⁸B. Ya. Kotyuzhanskii and L. A. Prozorova, *Zh. Eksp. Teor. Fiz.* **85**, 1461 (1983) [*Sov. Phys. JETP* **58**, 846 (1983)].

²⁹A. S. Borovik-Romanov, N. M. Kreines, and L. A. Prozorova, *ibid.* **45**, 64 (1963) [**18**, 46 (1964)].

³⁰V. I. Ozhogin and V. I. Preobrazhenskii, *ibid.* **73**, 988 (1977) [**45**, 523 (1977)].

³¹A. I. Smirnov, *ibid.* **84**, 2290 (1983) [**57**, 1335 (1983)].

³²B. Ya. Kotyuzhanskii and L. A. Prozorova, *ibid.* **86**, 658 (1984) [**59**, No. 2 (1984)].

³³A. A. Prozorova and A. I. Smirnov, *ibid.* **67**, 1952 (1974) [**40**, 970 (1974)].

Translated by J. G. Adashko